

Document downloaded from the institutional repository of the University of Alcalá: <https://ebuah.uah.es/dspace/>

This is a postprint version of the following published document:

López-López, M. et al., 2016. Surface-enhanced Raman spectroscopy for the analysis of smokeless gunpowders and macroscopic gunshot residues. *Analytical and bioanalytical chemistry*, 408(18), pp.4965-4973.

Available at <https://doi.org/10.1007/s00216-016-9591-z>

© 2016 Springer

*(Article begins on next page)*

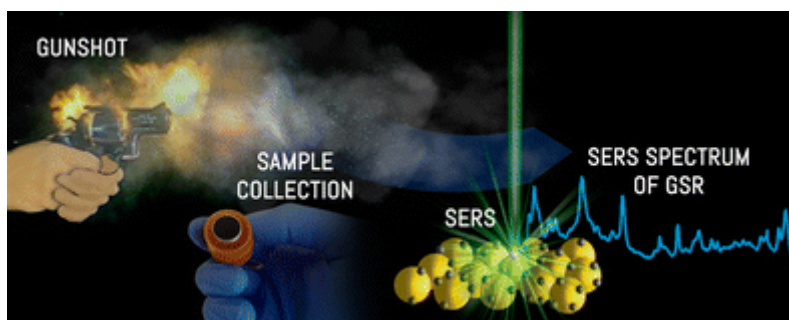


This work is licensed under a  
Creative Commons Attribution-NonCommercial-NoDerivatives  
4.0 International License.

# Surface-enhanced Raman spectroscopy for the analysis of smokeless gunpowders and macroscopic gunshot residues

María López López, Virginia Merk, Carmen García Ruiz, Janina Kneipp.

**Abstract:** Gunshot residues (GSR) result from the discharge of a firearm being a potential piece of evidence in criminal investigations. The macroscopic GSR particles are basically formed by burned and non-burned gunpowder. Motivated by the demand of trace analysis of these samples, in this paper, the use of surface-enhanced Raman scattering (SERS) was evaluated for the analysis of gunpowders and macroscopic GSR particles. Twenty-one different smokeless gunpowders were extracted with ethanol. SERS spectra were obtained from the diluted extracts using gold nanoaggregates and an excitation wavelength of 633 nm. They show mainly bands that could be assigned to the stabilizers diphenylamine and ethylcentralite present in the gunpowders. Then, macroscopic GSR particles obtained after firing two different ammunition cartridges on clothing were also measured using the same procedure. SERS allowed the detection of the particles collected with an aluminum stub from cloth targets without interferences from the adhesive carbon. The results demonstrate the great potential of SERS for the analysis of macroscopic GSR particles. Furthermore, they indicate that the grain-to-grain inhomogeneity of the gunpowders needs to be considered.



## 1. Introduction

Smokeless gunpowders are nitrocellulose-based propellants used in ammunition cartridges. Thus, they are commonly encountered in forensic laboratories either in the unburned form or in the burned form as a component of gunshot residues (GSR) [1]. In addition to offences related to firearms, they have been used in the construction of improvised explosive devices related to criminal acts [2]. Hence, the identification of compounds that can link the residue samples with unfired gunpowder provides valuable evidence to the forensic scientist.

Smokeless gunpowders are commonly classified according to their chemical composition, by the number of their primary energetic ingredients. Thus, propellants based on nitrocellulose are usually described as single-base gunpowders, mixtures of nitrocellulose with nitroglycerine are known as double-base gunpowders, and triple-base gunpowders present nitrocellulose, nitroglycerine, and nitroguanidine in their composition [3]. Additionally, they contain other compounds with different functions such as stabilizers, plasticizers, flash suppressants, deterrents, opacifiers, and dyes [4]. The determination of gunpowder compounds has so far been performed by different techniques such as thin-layer chromatography [5], high-performance liquid chromatography with UV absorbance detection [5–7] or hyphenated with electrospray ionization mass spectrometry [8], gas chromatography [9, 10], capillary electrophoresis [7], capillary electrochromatography (CEC) coupled to UV and time of flight-mass spectrometry (TOF-MS) [11], differential pulse polarography and squarewave voltammetry [6], ion mobility spectrometry (IMS) [2] and IMS combined with solid phase microextraction (SPME) [9, 12], and laser electrospray mass spectrometry (LEMS) [13].

Spectroscopic techniques, specifically infrared and Raman spectroscopy, enable a fast analysis of gunpowders with no or little sample preparation [1]. Several approaches based on both techniques were also used for the analysis of macroparticles of GSR, which basically consist of unburned gunpowder [14, 15], also in combination with discriminant analyses and other statistical tools [16, 17]. Imaging with microscopic-attenuated total reflectance (ATR)-FTIR [18] and Raman microspectroscopy [19, 20] allows to rapidly scan large areas of sample and detect GSR macroparticles, even when the particles are collected using standard SEM-EDX pin stubs [20], SEM-EDX being the method of choice in practice for the analysis of the GSR [21].

Surface-enhanced Raman scattering (SERS) is a very sensitive technique for the detection and characterization of molecules and molecular mixtures [22, 23]. It can enhance Raman signals from molecules that are in close proximity to a metal nanostructure by many orders of magnitude [24, 25]. The main contribution to the enhancement in SERS comes from the high local fields of localized surface plasmons in the metal nanostructures [22]. Motivated by the urgent demand for trace analysis of explosives, there are some reports in the literature concerning the use of SERS for the detection of trace amounts of explosives [26, 27]. Most of them focus on the detection of the common nitro aromatic explosives, e.g., di- and trinitrotoluene. In the work presented here, we pursued the analysis of gunpowders and GSR by SERS to achieve their fast and sensitive analysis. Specifically, 21 gunpowders of different composition and dates of manufacture were analyzed using gold nanoaggregates as SERS substrate and an excitation wavelength of 633 nm. The sensitivity and reproducibility of the method was investigated. Furthermore, GSR particles from real samples were analyzed. For a comprehensive evaluation of the potential of the proposed technique, we discuss here two approaches for sampling the GSR particles, using metal tweezers and diameter aluminum SEM/EDX stub with adhesive carbon, respectively.

## **2. Materials and methods**

### **Reagents and samples**

Gold (III) chloride trihydrate (99.9 %) and NaCl and ethanol (ACS reagent,  $\geq 99.5$  %) were purchased from Sigma-Aldrich (Taufkirchen, Germany) and trisodium citrate dihydrate (99 %) from Merck (Darmstadt, Germany). Diphenylamine (DPA), N-nitroso-DPA, 2-nitro-DPA, 2,4-dinitrotoluene, and ethylcentralite were kindly provided by “La Marañosa Institute of Technology” (ITM) (Madrid, Spain). Ultrapure water (18 M $\Omega$ ) was obtained from a Millipore Milli-Q gradient A10 water purification system from Millipore (Bedford, MA, USA). Twenty-one gunpowder samples were provided by Acuartelamiento San Juan del Viso (Madrid, Spain) (further details in Table 1).

**Table 1.** Smokeless gunpowder samples used in this study (composition and age were obtained from the labels provided by the respective manufacturer)

Sample/Year of manufacture	Composition
1/1987	Nitrocellulose $85 \pm 2$ %, diphenylamine 0.9–1.1 %, dinitrotoluene $10 \pm 2$ %, dibutyl phthalate $5 \pm 1$ %
2/1995	Nitrocellulose $85 \pm 2$ %, diphenylamine 0.9–1.1 %, dinitrotoluene $10 \pm 2$ %, dibutyl phthalate $5 \pm 1$ %
3/1991	Nitrocellulose $82 \pm 2$ %, nitroglycerin $12 \pm 2$ %, dibutyl phthalate $5 \pm 2.5$ %, diphenylamine $>1$ %, sodium sulfate $<0.3$ %, dinitrotoluene $<0.5$ %, potassium nitrate $<1$ %, calcium carbonate $<1$ %, graphite 0.05–0.2 %
4/1992	Nitrocellulose $85 \pm 2$ %, dinitrotoluene $10 \pm 2$ %, dibutyl phthalate $5 \pm 1$ %, diphenylamine $1 \pm 0.1$ %, potassium sulfate $0.5 \pm 2$ %
5/1989	Nitrocellulose $94.0 \pm 1.5$ %, ethylcentralite $1.9 \pm 0.3$ %, diphenylamine $1.0 \pm 0.2$ %, dibutyl phthalate $1.9 \pm 0.3$ %, sodium oxalate $0.5 \pm 0.2$ %, potassium sulfate $0.7 \pm 0.3$ %, graphite $<0.5$ %
6/1998	Nitrocellulose $85 \pm 2$ %, diphenylamine 0.9–1.1 %, dinitrotoluene $10 \pm 2$ %, dibutyl phthalate $5 \pm 1$ %
7/1985	Nitrocellulose $57.30 \pm 0.3$ %, nitroglycerin $41.5 \pm 0.3$ %, diphenylamine 0.67 %, centralite 0.33 %, graphite 0.20 %
8/1998	Nitrocellulose $57.30 \pm 0.3$ %, nitroglycerin $40.7 \pm 2.2$ %, diphenylamine $>0.44$ %, centralite $>0.44$ %, graphite $<0.20$ %
9/1998	Nitrocellulose $67.10 \pm 1.6$ %, nitroglycerin $28.9 \pm 0.75$ %, centralite $2.0 \pm 0.2$ %, dibutyl phthalate $4.0 \pm 0.4$ %
10/1997	Nitrocellulose $82 \pm 2$ %, nitroglycerin $12 \pm 2$ %, dibutyl phthalate $5 \pm 2.5$ %, diphenylamine $1.4 \pm 0.2$ %, sodium sulfate $<0.3$ %, dinitrotoluene $<0.5$ %, potassium nitrate $<1$ %, graphite 0.2–0.1 %
11/1991	Nitrocellulose $71.0 \pm 3.0$ %, nitroglycerin $25.0 \pm 2$ %, ethylcentralite $3.0 \pm 1.0$ %, graphite $0.2 \pm 0.1$ %, potassium nitrate $<1.25$ %
12/1982	Nitrocellulose 54.5 %, nitroglycerin 35.5 %, potassium perchlorate, carbon black and centralite 10 %

13/1996 Nitrocellulose  $85 \pm 2$  %, diphenylamine 0.9–1.1 %, dinitrotoluene  $10 \pm 2$  %, dibutyl phthalate  $5 \pm 1$  %

14/1984 Nitrocellulose  $85 \pm 2$  %, diphenylamine 0.9–1.1 %, dinitrotoluene  $10 \pm 2$  %, dibutyl phthalate  $5 \pm 1$  %

15/1994 Nitrocellulose  $82 \pm 2$  %, nitroglycerin  $12 \pm 2$  %, dibutyl phthalate  $5 \pm 2$  %, diphenylamine  $1.4 \pm 0.2$  %, sodium sulfate  $<0.5$  %, dinitrotoluene  $<0.5$  %, potassium nitrate  $<1$  %, graphite 0.2–0.1 %

16/1980 Nitrocellulose  $85 \pm 2$  %, dinitrotoluene  $10 \pm 2$  %, dibutyl phthalate  $5 \pm 1$  %, diphenylamine  $1 \pm 0.1$  %, potassium sulfate  $0.6 \pm 0.2$  %

17/1990 Nitrocellulose  $94.0 \pm 1.5$  %, ethylcentralite  $1.9 \pm 0.3$  %, diphenylamine  $1.0 \pm 0.2$  %, dibutyl phthalate  $1.9 \pm 0.3$  %, sodium oxalate  $0.5 \pm 0.2$  %, potassium sulfate  $0.7 \pm 0.3$  %, graphite  $<0.5$  %

18/1991 Nitrocellulose  $94.0 \pm 1.5$  %, ethylcentralite  $1.9 \pm 0.3$  %, diphenylamine  $1.0 \pm 0.2$  %, dibutyl phthalate  $1.9 \pm 0.3$  %, sodium oxalate  $0.5 \pm 0.2$  %, potassium sulfate  $0.7 \pm 0.3$  %, graphite  $<0.5$  %

19/Unknown Nitrocellulose  $87 \pm 2$  %, diphenylamine  $1.05 \pm 0.15$  %, potassium sulfate  $0.5 \pm 0.25$  %, dinitrotoluene  $10.00 \pm 2$  %, dibutyl phthalate  $3.00 \pm 0.5$  %, graphite  $87 \pm 2$  %

20/1984 Nitrocellulose  $57.30 \pm 0.3$  %, nitroglycerin  $41.5 \pm 0.3$  %, diphenylamine 0.67 %, centralite 0.33 %, graphite 0.20 %

21/1980 Nitrocellulose 100 %, diphenylamine 0.90–1.15 %, potassium sulfate  $0.6 \pm 0.10$  %

Super X 0.22 in. from Western Cartridge Company (East Alton, United States) and GFL 38sp 0.38 in. from Giulio Fiocchi s.p.a. (Lecco, Italy) ammunition cartridges were fired over white cotton cloths (20 × 20 cm) fixed in cardboards to obtain the GSR particles. The shoots were fired at a perpendicular angle to the targets, and the firing distance was set at approximately 1 m. The shoots were performed at the shooting range of the Criminalistic Service of Guardia Civil (Madrid, Spain).

## **Nanoparticle synthesis and characterization**

According to [28], 200 mL of 0.375 mM gold (III)chloride trihydrate solution were brought to boiling. Then, a 1 % trisodium citrate dehydrate solution was added and boiled for further 30 min. The heat source was removed, and the solution was stirred for 1 h at room temperature. For all experiments, ultrapure water (18 M $\Omega$ ) was used.

Extinction spectra of gold nanoparticles were recorded with a V-670 double-beam ultraviolet-visible (UV-vis)/near-infrared (NIR) spectrophotometer (JASCO, Gross-Umstadt, Germany) and show a plasmon band with a maximum at 526 nm.

## **Sample preparation**

Figure 1 depicts a scheme that summarizes the sample preparation performed in the present work. Approximately 4 mg of gunpowder was extracted with ethanol (10  $\mu$ L) in an ultrasonic bath for 15 min at 35 °C. Twenty-seven microliters of ultrapure water was added to 3  $\mu$ L of the ethanolic extracts. Then, 2  $\mu$ L of these solutions was added to 20  $\mu$ L of gold nanoparticles. Finally, a drop of the nanoparticle solution was placed on a CaF<sub>2</sub> slide (see Fig. 1(I)). In order to evaluate the reproducibility of the method, two gunpowders (samples 19 and 20, see Table 1) were extracted four times and analyzed. Additionally, the effect of the gunpowder concentration was evaluated. For this purpose, four samples (samples 4, 10, 18, and 20, see Table 1) were extracted. Water dilutions were made from the ethanol extracts and then mixed with the gold nanoparticles, obtaining gold nanoparticle solutions with concentrations of gunpowder of approximately 3.3, 0.33, 0.17, 0.033, and 0.003  $\mu$ g/ $\mu$ L.

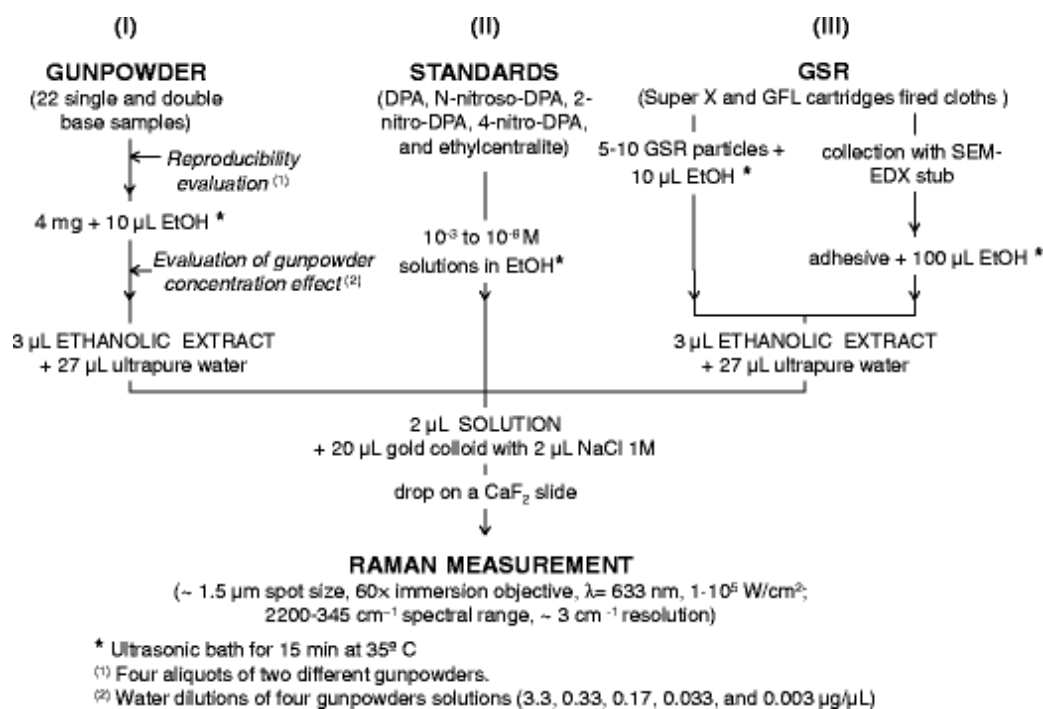


**Figure 1.** Experimental scheme for sample preparation.

Concentrations from 10<sup>-3</sup> to 10<sup>-8</sup> M of DPA, N-nitroso-DPA, 2-nitro-DPA, 4-nitro-DPA, and ethylcentralite in gold nanoparticle solution (2 µL of standard solution, 20 µL of gold nanoparticles) were prepared by prior dissolution of the standards in ethanol.

Two approaches were performed for the preparation of the macroscopic GSR particles (see Fig. 1(III)). The target cloths were placed under a stereo microscope Motic SMZ-168 TL (Motic, Hong Kong, China), and 5 to 10 macroscopic GSR particles of each fired ammunition were collected using metal tweezers previously cleaned with acetone. The particles were collected approximately 10 cm in diameter around the entrance hole. Particles were introduced into Eppendorf tubes, and 10 µL of ethanol was added to extract the GSR compounds. Then, 3 µL of the extract was added to 27 µL of ultrapure water. Two microliters of this solution was added to 20 µL of gold nanoparticles. Finally, a drop of this solution was placed on a CaF<sub>2</sub> slide.

Additionally, a 13-mm-diameter aluminum stub with adhesive carbon for SEM-EDX analysis was used to collect the particles from the cloth targets. The SEM-EDX stub was pressed 20 times over the clothing (in the area at approximately 10 cm in diameter around the entrance hole), causing the transferring of the GSR particles to the adhesive tape. Then, the adhesive sticker was removed from the aluminum stub and cut into small pieces. The pieces were introduced into an Eppendorf tube, and 100 µL of ethanol was added to extract the GSR compounds. Three microliters of the extract was added to 27



$\mu\text{L}$  of ultrapure water. Two microliters of this solution was added to 20  $\mu\text{L}$  gold nanoparticles. Finally, a drop of this solution was placed on a  $\text{CaF}_2$  slide. The same procedure was performed using a clean adhesive carbon for SEM-EDX analysis to visualize the possible bands coming from the adhesive (blank sample).

## **Instrumentation**

A Raman microscope equipped with a  $\times 60$  immersion objective (Olympus, 1.5- $\mu\text{m}$  spot diameter), a nitrogen-cooled CCD camera (Horiba Jobin Yvon), and a 633-nm helium-neon-laser (Thorlabs, HRP 170) was used. The excitation power at the sample was about  $1 \cdot 10^5 \text{ W/cm}^2$ . SERS spectra were recorded between 2200 and  $345 \text{ cm}^{-1}$  at a resolution of  $\sim 3 \text{ cm}^{-1}$ .

## **3. Results and discussion**

The 21 gunpowders used in this work are detailed in Table 1. The samples, with different composition, are single-base gunpowders (nitrocellulose only as active component) and double-base gunpowders (nitrocellulose and nitroglycerine as primary energetic ingredients) [1, 3, 29]. The samples contain several additives, e.g., plasticizers such as dinitrotoluene or dibutyl phthalate, and stabilizers such as diphenylamine (DPA) or ethylcentralite. Those stabilizers, especially DPA, added to gunpowders to stop the decomposition of the original compounds, can degrade with time and form new compounds [3]. Therefore, the date of manufacture is also given in Table 1.

### **SERS-based distinction of gunpowders with different stabilizers**

The SERS spectra of the gunpowders were acquired with gold nanoparticles (experimental procedure in Fig. 1(I)). DPA and ethylcentralite are the main stabilizers for smokeless gunpowders. The presence or absence of these two compounds can be used to distinguish different gunpowders, although the discriminating power is low. Taking DPA as an example, and considering 1 % (m/m) of DPA in the gunpowder and a total extraction of the DPA, the concentration of DPA in the extract would be about  $10^{-4} \text{ M}$ . However, it is probable that, due to DPA degradation, the final concentration of DPA in the nanoparticle solution is lower than  $10^{-4} \text{ M}$ .

Figure 2a shows the SERS spectra of five smokeless gunpowders that all contain DPA as stabilizer but differ in the composition of the other additives (see Table 1). A comparison of the spectra shows several differences but also that some bands appear in all the spectra (e.g., 1581, 1359, 1175, and 407  $\text{cm}^{-1}$ ).

Figure 1. a Comparison of SERS spectra of five smokeless gunpowders with DPA (see Table 1); b SERS spectra of DPA, DPA derivatives, and a mixture of DPA and its derivatives: DPA,  $5 \cdot 10^{-5}$  M; N-nitroso-DPA,  $1.6 \cdot 10^{-5}$  M; 2-nitro-DPA and 4-nitro-DPA,  $8.3 \cdot 10^{-6}$  M. Raman conditions: excitation at 633 nm,  $1 \cdot 10^5$  W/cm<sup>2</sup>, acquisition time of 1 s (gunpowders) and 10 s (DPA standards). Several bands are labeled for clarity.

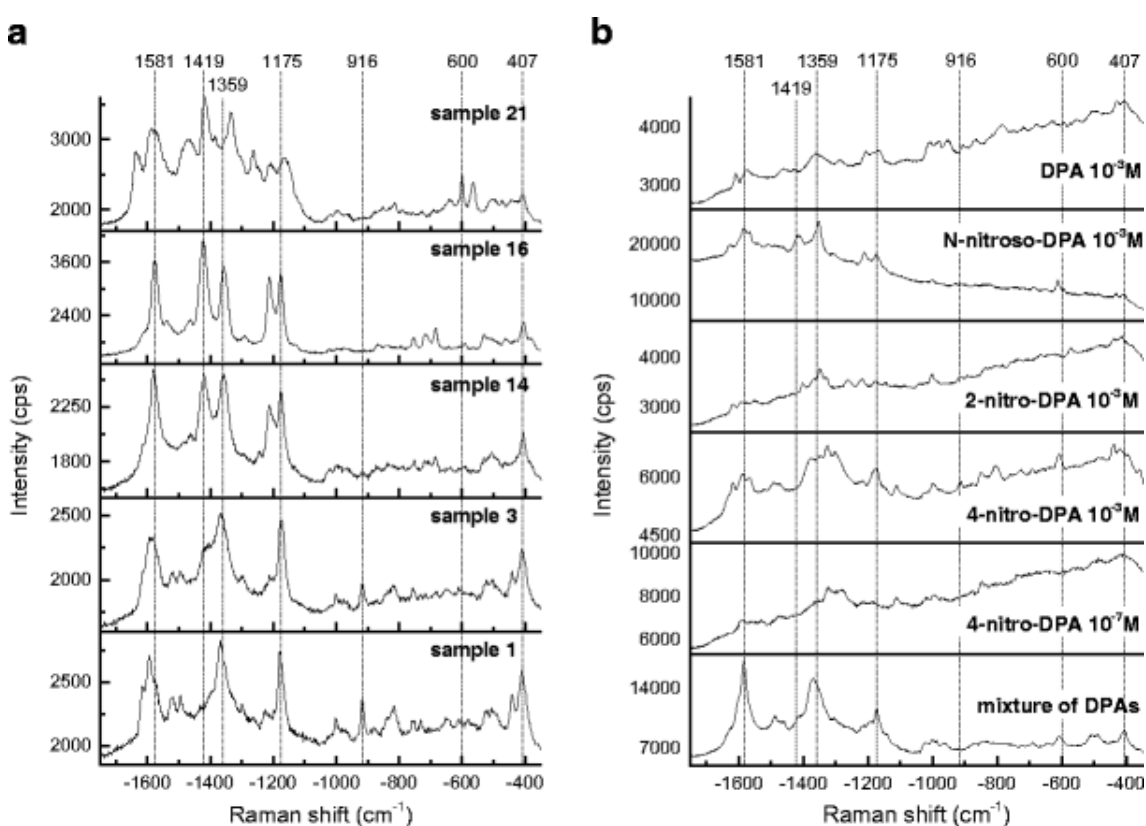
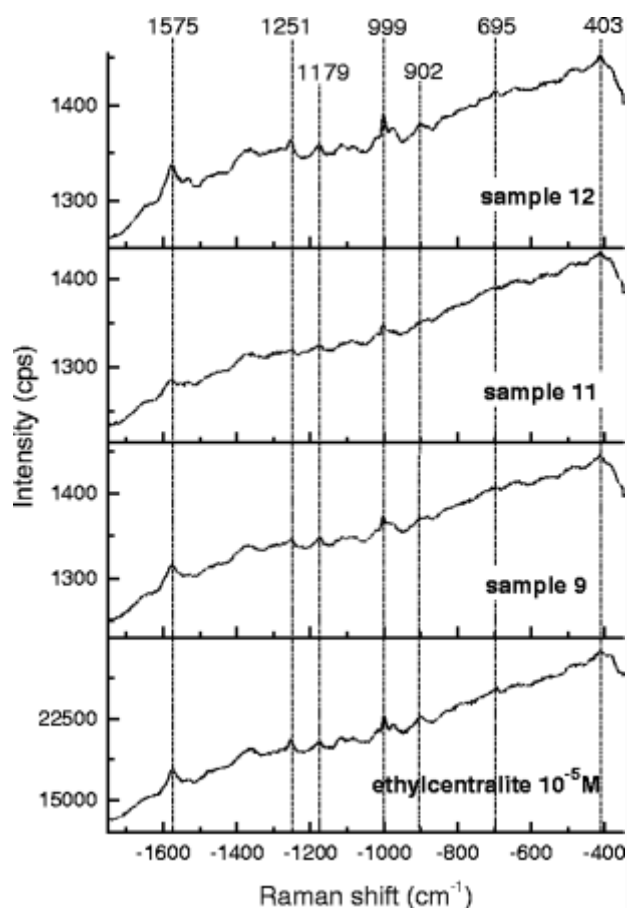


**Figure 2.** a Comparison of SERS spectra of five smokeless gunpowders with DPA (see Table 1); b SERS spectra of DPA, DPA derivatives, and a mixture of DPA and its derivatives: DPA,  $5 \cdot 10^{-5}$  M; N-nitroso-DPA,  $1.6 \cdot 10^{-5}$  M; 2-nitro-DPA and 4-nitro-DPA,  $8.3 \cdot 10^{-6}$  M. Raman conditions: excitation at 633 nm,  $1 \cdot 10^5$  W/cm<sup>2</sup>, acquisition time of 1 s (gunpowders) and 10 s (DPA standards). Several bands are labeled for clarity.

To assign the bands observed, SERS spectra of DPA and some of its derivatives that can result from the degradation of DPA by different pathways [3] were measured. Figure 2b depicts the spectra of DPA, N-nitroso-DPA, 2-nitro-DPA, 4-nitro-DPA, and a mixture of them. The interaction of a molecular species and/or the nanoparticles with other molecules plays a critical role, reflecting, e.g., in a concentration dependence of the SERS spectra [30, 31]. The orientation of the analyte molecules can have a strong influence on the bands observed in the spectrum [32]. Therefore, also mixtures of DPA and its derivatives were measured with SERS. SERS spectra were observed for a concentration of DPA as low as  $10^{-6}$  M and of the nitrated derivatives of  $10^{-7}$  M (Fig. 2b). Comparison of these spectra with those of the DPA-containing gunpowders (Fig. 2a) provides evidence that most bands that occur in all spectra of the different gunpowders can be attributed to DPA and its derivatives. In fact, the spectrum of the DPA's mixture (bottom trace in Fig. 2b) is the most similar to the gunpowder spectra. No relationship between the date of manufacturing and the spectra obtained was observed.

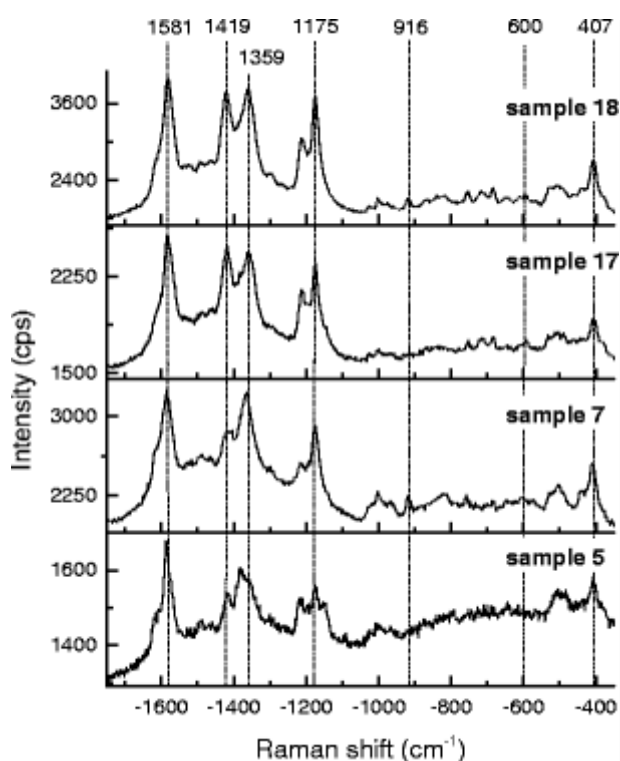
Several of the gunpowders analyzed contain dinitrotoluene. Due to the great number of papers present in the scientific literature that deal with the SERS analysis of 2,4-dinitrotoluene (see, e.g., references [33–35]), we expected to observe additional bands in the SERS spectra of the gunpowders containing this compound. However, when we analyzed a  $10^{-3}$  M 2,4-dinitrotoluene, we only observed very weak bands at about 1581, 1533, 1334, and 998  $\text{cm}^{-1}$  (data not shown). These bands were not observed in the spectra of the gunpowders with 2,4-dinitrotoluene, probably because they are overlaid by bands from other compounds present in the gunpowder formulation.

Figure 3 displays the SERS spectra obtained for three smokeless gunpowders with ethylcentralite (samples 9, 11, and 12, see Table 1) and an ethylcentralite standard. The SERS spectrum for the ethylcentralite standard was observed at concentrations as low as  $10^{-6}$  M. As is evidenced by the comparison with the standard, the bands observed in the SERS spectra of these gunpowders can be attributed to ethylcentralite. Assuming 3 % (m/m) of ethylcentralite in the gunpowder and a complete extraction, the ethylcentralite concentration in the gold colloid can be estimated to be around  $10^{-4}$  M. No ethylcentralite degradation was taken into account for this estimation.



**Figure 3.** Comparison among the SERS spectra of three smokeless gunpowders with ethylcentralite and the SERS spectrum of ethylcentralite. a Sample 12, b sample 11, c sample 9, and d ethylcentralite  $10^{-5}$  M (see Table 1). Raman conditions: excitation at 633 nm,  $1 \cdot 10^5$  W/cm<sup>2</sup>, acquisition time of 60 s. Several bands are labeled for clarity.

There are some gunpowders containing both DPA and ethylcentralite as stabilizers. Figure 4 shows the spectra of four of these smokeless gunpowders (samples 5, 7, 17, and 18, please refer to Table 1). The spectra obtained are similar to those observed for the gunpowders with DPA (Fig. 2a). This indicates that the signals of the ethylcentralite are overlaid by the ones from the DPA, or the interaction of DPA with the gold nanoparticle surface is favored over the one with ethylcentralite.



**Figure 4.** SERS spectra of four smokeless gunpowders with DPA and ethylcentralite (see Table 1). Raman conditions: excitation at 633 nm,  $1 \cdot 10^5$  W/cm<sup>2</sup>, acquisition time of 1 s. Several bands are labeled for clarity.

In order to investigate if the SERS spectrum of a gunpowder can be used for identification purposes, the reproducibility and sensitivity of the method, as well as the effect of the sample dilution on the SERS spectra, were studied.

To evaluate the reproducibility of the method, four aliquots of two different gunpowders (samples 19 and 20 in Table 1) were extracted using the procedure described above. Figure 5 depicts the SERS spectra of the mentioned extractions. As can be seen, the spectra obtained from different preparations of sample 19 (Fig. 5a) show several qualitative differences, e.g., in the relative intensity in the band at about 1419 cm<sup>-1</sup>, while sample 20 (Fig. 5b) shows the same spectrum for all four extractions, in spite of different absolute intensities and varying background signals. No differences were observed for the different spectra taken from the same extract; therefore, the spectral differences observed among aliquots can probably be attributed to inhomogeneity of the gunpowder grains, leading to non-reproducible extraction.

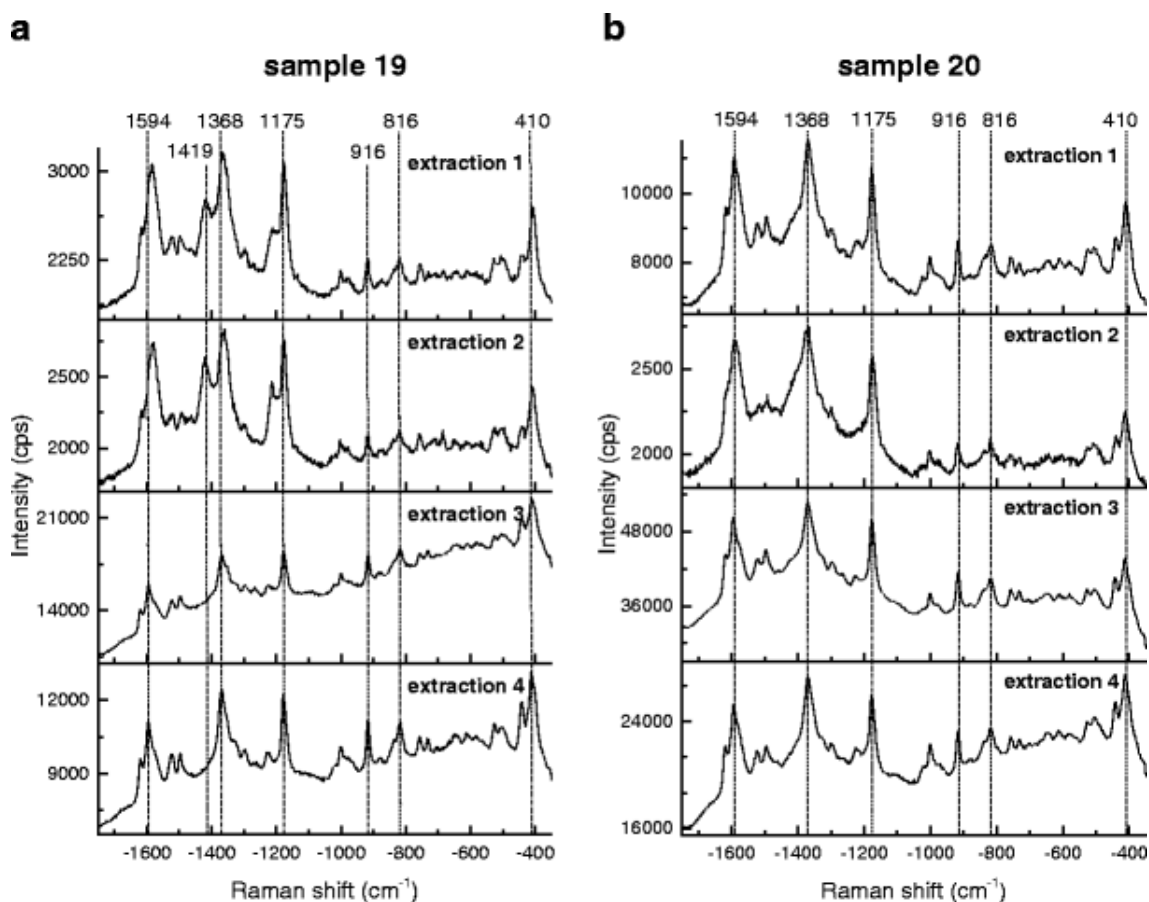


**Figure 5.** Comparison among the SERS spectra of the four extractions performed for **a** sample 19 and **b** sample 20 (see Table 1). Raman conditions: excitation at 633 nm,  $1 \cdot 10^6 \text{ W/cm}^2$ , acquisition time of 10 s. Several bands are labeled for clarity.

As another important aspect, the effect of the gunpowder concentration in the gold nanoparticle solutions was evaluated. For this purpose, four samples (samples 4, 10, 18, and 20, see Table 1) were extracted. Water dilutions were made from the ethanol extracts, obtaining gold colloids with concentrations of gunpowder of 3.3, 0.33, 0.17, and 0.003  $\mu\text{g}/\mu\text{L}$ . As stated above, these concentrations are roughly estimated due to the insolubility of the nitrocellulose. Figure 6 shows the SERS spectra obtained for two of the gunpowders (samples 10 and 20, see Table 1) at the above-mentioned concentrations. For all samples, the SERS spectra could be obtained down to a concentration of 0.033  $\mu\text{g}/\mu\text{L}$ . For the lowest concentration (0.003  $\mu\text{g}/\mu\text{L}$ ) no signals were observed and the spectra are therefore not shown. The spectra display predominantly the same bands for all concentrations, but the intensity ratio changes with concentration.

As discussed above, the interaction of a molecule with a metal nanostructure surface can change with the concentration of the analyte in solution [30, 36]. Since the SERS enhancement for individual vibrational modes of a molecule are also discussed in the context of the orientation of the molecule [32, 37], relative band ratios in the SERS spectrum can change with concentration. Nevertheless, most of the bands can be attributed to DPA and its derivatives.

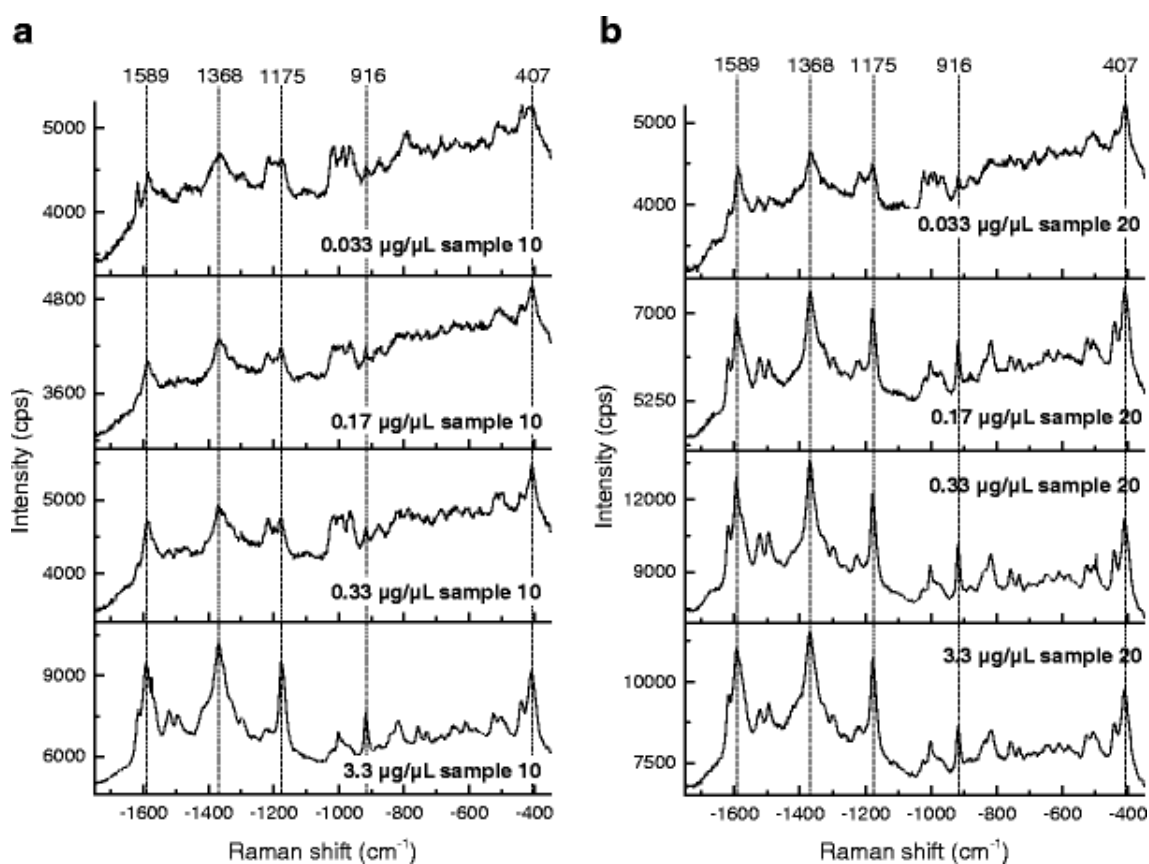


**Figure 6.** SERS spectra of two gunpowders at four different dilutions, a sample 10 and b sample 20 (see Table 1). Raman conditions: excitation at 633 nm,  $1 \cdot 10^5 \text{ W}/\text{cm}^2$ , acquisition time of 10 s. Several bands are labeled for clarity.

### SERS spectra from GSR

GSR macroparticles are basically formed by non-burned gunpowder [14]; as a consequence, the analysis of GSR by SERS was explored here as well. Two sampling methods were investigated (please refer to Fig. 1(III)) in order to evaluate the use of SERS for the analysis of GSR particles. The first method was based on the analysis of 5 to 10 GSR particles picked up with tweezers, extracted with ethanol, and then the

extract being analyzed by SERS. As the SERS analysis of them did not yield meaningful results, probably due to an insufficient amount of sample, a second approach was followed. In this sampling procedure, adhesive items, e.g., SEM-EDX stubs, were used to dab the clothing. Such adhesives are commonly used by the forensic investigators to collect GSR particles in the suspects (e.g., in the face, hair, hands, clothing, or other objects susceptible to present GSR particles), not in targets. The collected particles were extracted from the SEM-EDX stubs and SERS spectra were obtained. The same procedure was performed for a clean, double-coated adhesive of a SEM-EDX stub (blank sample). Figure 7 shows the SERS spectra of two smokeless gunpowders (samples 4 and 18, see Table 1) at a concentration of 0.033  $\mu\text{g}/\mu\text{L}$  and the spectra of the GSR extracted from the SEM-EDX stubs. Although the spectrum of the clean double-coated adhesive shows two small additional bands at about 1534 and 996  $\text{cm}^{-1}$  that can be assigned to constituents of the adhesive, they did not interfere in the identification of the GSR. The SERS spectra of the GSR are very similar to the SERS spectra of the diluted gunpowders and to the spectrum of DPA. This confirms that GSR can be analyzed by SERS and the same stubs used for SEM-EDX can be used for the SERS analysis.

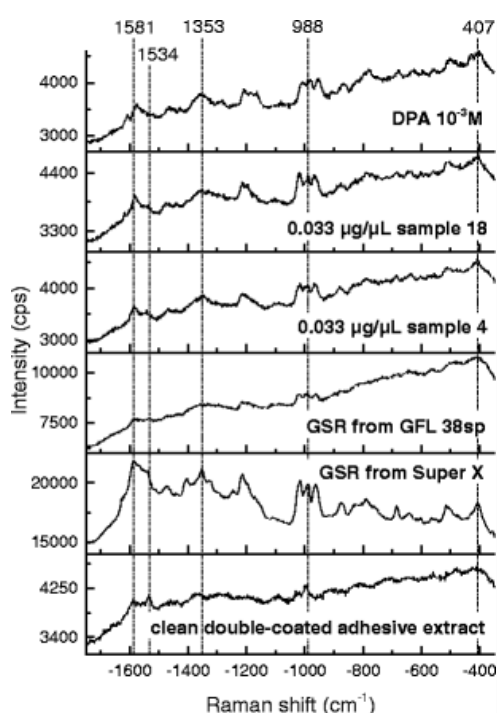


**Figure 7.** SERS spectra of DPA  $10^{-3}$  M, sample 18 (0.033  $\mu\text{g}$  gunpowder/ $\mu\text{L}$ ), sample 4 (0.033  $\mu\text{g}$  gunpowder/ $\mu\text{L}$ ), GSR from GFL 38sp ammunition, GSR from Super X ammunition, and clean double-coated adhesive extract (see Table 1). Raman conditions: excitation at 633 nm,  $1 \cdot 10^5$  W/ $\text{cm}^2$ , acquisition time of 10 s for all samples except for the GSR SERS spectra (60 s). Several bands are labeled for clarity.



## 4. Conclusions

The analysis of 21 different smokeless gunpowders as well as their most common stabilizers was performed by SERS. The SERS spectra of the stabilizers were observed for a concentration of DPA and ethylcentralite as low as  $10^{-6}$  M and for the DPA-nitrated derivatives as low as  $10^{-7}$  M. The gunpowders give SERS spectra that show mainly bands that could be assigned to the stabilizers ethylcentralite, DPA, and DPA derivatives even when other compounds are present (such as dinitrotoluene or nitroglycerin). The gunpowders with DPA show intense spectra that allow their identification at a low concentration of gunpowder ( $\sim 0.033$   $\mu\text{g}/\mu\text{L}$  of gunpowder, which corresponds to  $\sim 0.3$   $\text{ng}/\mu\text{g}$  of DPA). Nevertheless, gunpowders with ethylcentralite show weaker SERS spectra. In addition to the mentioned increase of sensitivity, SERS has the benefit of avoiding the microscopic localization required using Raman microspectroscopy.

On the other hand, the high sensitivity of SERS allowed the detection of GSR collected with SEM-EDX stub from cloth targets shot at close distance. However, the use of this technique of preparation presents the disadvantage of destroying the sample, not allowing additional analyses on the sample. Additionally, for a practical application, the inherent grain-to-grain inhomogeneity of the gunpowders could be a limiting factor to unequivocally link a GSR macroparticle with ammunition and should be considered. Also, DPA is present in the environment and could lead to false positives.

## Acknowledgments

V.M. and J.K. would like to acknowledge the support by ERC Starting Grant 259432. M. López-López and C. García-Ruiz thank the European Commission for the Project HOME/2011/ISEC/AG/4000002480 accomplished with the financial support of the Prevention of and Fight against Crime Programme European Commission—Directorate—General Home Affairs. This project has been funded with the support from the European Commission. This publication reflects the views of the author, and the European Commission cannot be held responsible for any use which may be made of the information contained therein. M. López-López thanks the Spanish Ministry of Education, Culture and Sports for the José Castillejo mobility grant. V.M. acknowledges the support by the project DFG GSC 1013 (SALSA).

## References

1. Scherperel G, Reid GE, Smith RW. Characterization of smokeless powders using nanoelectrospray ionization mass spectrometry (nESI-MS). *Anal Bioanal Chem.* 2009;294:2019–28.
2. West C, Baron G, Minet JJ. Detection of gunpowder stabilizers with ion mobility spectrometry. *Forensic Sci Int.* 2007;166:91–101.
3. López-López M, Bravo JC, García-Ruiz C, Torre M. Diphenylamine and derivatives as predictors of gunpowder age by means of HPLC and statistical models. *Talanta.* 2013;103:214–20.
4. López-López M, Fernández MA, Sáiz J, Ferrando JL, Vega A, Torre M, et al. New protocol for the isolation of nitrocellulose from gunpowders: utility in their identification. *Talanta.* 2010;81:1742–9.
5. Espinoza EO'N, Thornton JI. Characterization of smokeless gunpowder by means of diphenylamine stabilizer and its nitrated derivatives. *Anal Chim Acta.* 1994;288:57–69.
6. Pérez A, Tascón ML, Vázquez MD, Batanero PS. Polarographic study on the evolution of the diphenylamine as stabiliser of the solid propellants. *Talanta.* 2004;62:165–73.
7. MacCrehan WA, Bedner M. Development of a smokeless powder reference material for propellant and explosives analysis. *Forensic Sci Int.* 2006;163:119–24.
8. Mathis JA, McCord BR. Gradient reversed-phase liquid chromatographic-electrospray ionization mass spectrometric method for the comparison of smokeless powders. *J Chromatogr A.* 2003;988:107–16.
9. Joshi M, Rigsby K, Almirall JR. Analysis of the headspace composition of smokeless powders using GC-MS, GC- $\mu$ ECD and ion mobility spectrometry. *Forensic Sci Int.* 2011;208:29–36.
10. Sharma SP, Lahiri SC. A preliminary investigation into the use of FTIR microscopy as a probe for the identification of bullet entrance holes and the distance of firing. *Sci Justice.* 2009;49:197–204.

11. de Perre C, Corbin I, Blas M, McCord BR. Separation and identification of smokeless gunpowder additives by capillary electrochromatography. *J Chromatogr A*. 2012;1267:259–65.
12. Joshi M, Delgado Y, Guerra P, Lai H, Almirall JR. Detection of odor signatures of smokeless powders using solid phase microextraction coupled to an ion mobility spectrometer. *Forensic Sci Int*. 2009;188:112–8.
13. Perez JJ, Flanigan PM, Brady JJ, Levis RJ. Classification of smokeless powders using laser electrospray mass spectrometry and offline multivariate statistical analysis. *Anal Chem*. 2013;85:296–302.
14. López-López M, Delgado JJ, García-Ruiz C. Analysis of macroscopic gunshot residues by Raman spectroscopy to assess the weapon memory effect. *Forensic Sci Int*. 2013;231:1–5.
15. López-López M, Delgado JJ, García-Ruiz C. Ammunition identification by means of the organic analysis of gunshot residues using Raman spectroscopy. *Anal Chem*. 2012;84:3581–5.
16. Bueno J, Sikirzhyski V, Lednev I. Raman spectroscopic analysis of gunshot residue offering great potential for caliber differentiation. *Anal Chem*. 2012;84:4334–9.
17. Bueno J, Lednev IK. Advanced statistical analysis and discrimination of gunshot residue implementing combined Raman and FT-IR Data. *Anal Methods*. 2013;5:6292–6.
18. Bueno J, Lednev IK. Attenuated total reflectance-FT-IR imaging for rapid and automated detection of gunshot residue. *Anal Chem*. 2014;86:3389–96.
19. Bueno J, Lednev IK. Raman microspectroscopic chemical mapping and chemometric classification for the identification of gunshot residue on adhesive tape. *Anal Bioanal Chem*. 2014;406:4595–9.
20. López-López M, Fernández MA, García-Ruiz C. Fast analysis of complete macroscopic gunshot residues on substrates using Raman imaging. *Appl Spectrosc*. 2015;69:889–93.
21. Brozek-Mucha Z. Comparison of cartridge case and airborne GSR—a study of the elemental composition and morphology by means of SEM-EDX. *X-Ray Spectrom*. 2007;36:398–407.

22. Kneipp K, Kneipp H, Kneipp J. Surface-enhanced Raman scattering in local optical fields of silver and gold nanoaggregates—from single-molecule Raman spectroscopy to ultrasensitive probing in live cells. *Acc Chem Res.* 2006;39:443–50.
23. Graham D, Goodacre R. Chemical and bioanalytical applications of surface enhanced Raman scattering spectroscopy. *Chem Soc Rev.* 2008;37:883–4.
24. Kneipp K, Wang Y, Kneipp H, Perelman LT, Itzkan I, Dasari RR, et al. Single molecule detection using surface-enhanced Raman scattering (SERS). *Phys Rev Lett.* 1997;78:1667–70.
25. Nie SM, Emory SR. Probing single molecules and single nanoparticles by surface-enhanced Raman scattering. *Science.* 1997;275:1102–6.
26. López-López M, García-Ruiz C. Infrared and Raman spectroscopy techniques applied to identification of explosives. *Trends Anal Chem.* 2014;54:36–44.
27. Hakonen A, Andersson PO, Schmidt MS, Rindzevicius T, Käll M. Explosive and chemical threat detection by surface-enhanced Raman scattering: a review. *Anal Chim Acta.* 2015;893:1–13.
28. Tkachenko A, Xie H, Franzen S, Feldheim DL. Assembly and characterization of biomolecule-gold nanoparticle conjugates and their use in intracellular imaging. *Methods Mol Biol.* 2005;303:85–99.
29. López-López M, Ferrando JL, García-Ruiz C. Comparative analysis of smokeless gunpowders by Fourier transform infrared and Raman spectroscopy. *Anal Chim Acta.* 2012;717:92–9.
30. Michota A, Bukowska J. Surface-enhanced Raman scattering (SERS) of 4-mercaptobenzoic acid on silver and gold substrates. *J Raman Spectrosc.* 2003;34:21–5.
31. Cañamares MV, García-Ramos JV, Domingo C. Surface-enhanced Raman scattering study of the adsorption of the anthraquinone pigment alizarin on Ag nanoparticles. *J Raman Spectrosc.* 2004;35:921–7.
32. Creighton JA. Surface Raman electromagnetic enhancement factors for molecules at the surface of small isolated metal spheres: The determination of adsorbate orientation from SERS relative intensities. *Surf Sci.* 1983;124:209–19.

33. Khaing MK, Chang CF, Sun Y, Fan X. Rapid, sensitive DNT vapor detection with UV-assisted photo-chemically synthesized gold nanoparticle SERS substrates. *Analyst*. 2011;136:2811–7.
34. Gong Z, Du H, Cheng F, Wang C, Wang C, Fan M. Fabrication of SERS swab for direct detection of trace explosives in fingerprints. *ACS Appl Mater Interfaces*. 2014;6:21931–7.
35. Sylvia JM, Janni JA, Klein JD, Spencer KM. Surface-enhanced Raman detection of 2,4-dinitrotoluene impurity vapor as a marker to locate landmines. *Anal Chem*. 2000;72:5834–40.
36. Corrigan DS, Weaver MJ. Coverage-dependent orientation of adsorbates as probed by potential-difference infrared spectroscopy: azide, cyanate, and thiocyanate at silver electrodes. *J Phys Chem*. 1986;90:5300–6.
37. Moskovits M, DiLella DP, Maynard KJ. Surface Raman spectroscopy of a number of cyclic aromatic molecules adsorbed on silver: selection rules and molecular reorientation. *Langmuir*. 1988;4:67–76.